Supporting Information

Designing of Novel Zinc(II) Schiff Base Complexes Having Acyl Hydrazone Linkage: Study of Phosphatase and Anti-Cancer Activity

Sanchari Dasgupta,[a] Suhana Karim,[a] Saswati Banerjee,[b] Moumita Saha,[b] Krishna Das Saha,[b] Debasis Das*,[a]

[a]Department of Chemistry, University of Calcutta, 92 A. P. C. Road, Kolkata 700009, India, E-mail: dasdebasis2001@yahoo.com

[b]Cancer Biology and Inflammatory Disorder Division, CSIR - Indian Institute of Chemical Biology, 4, Raja S C Mullick Road, Jadavpur, Kolkata-700032.

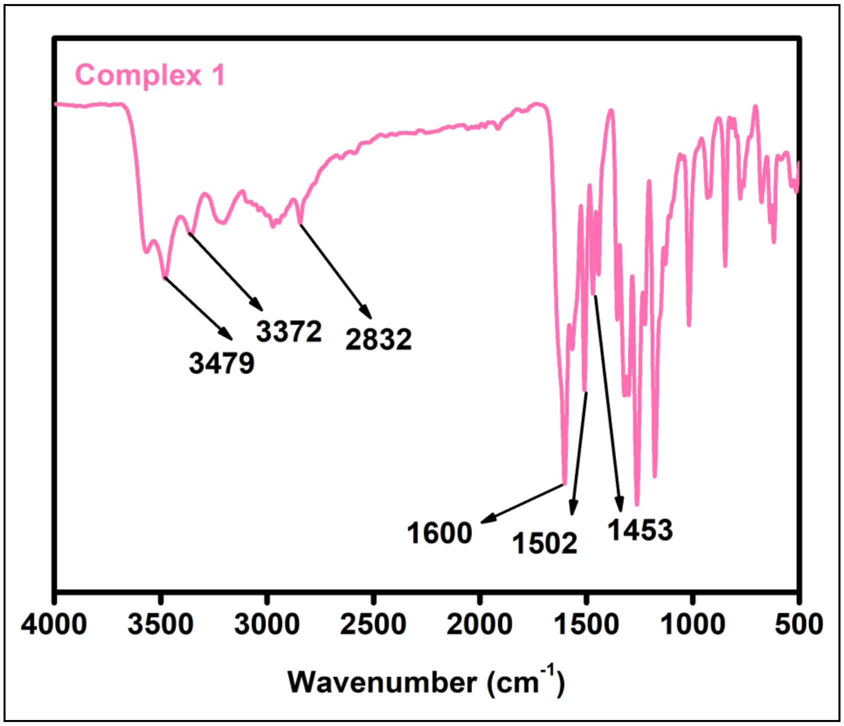

Fig. S1 FT-IR spectrum of complex **1.**

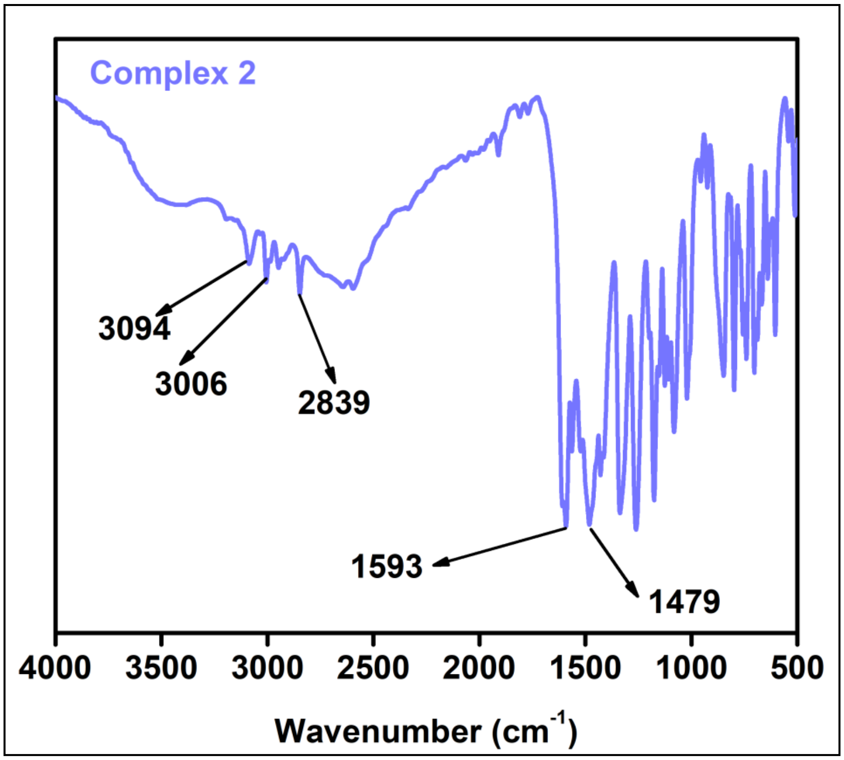

Fig. S2 FT-IR spectrum of complex **2.**

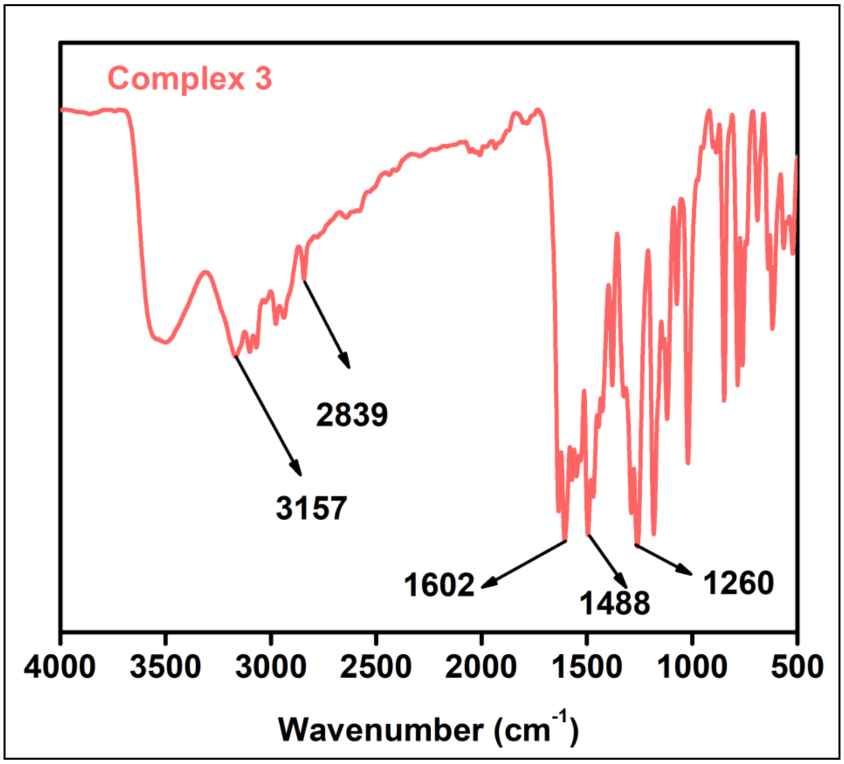

Fig. S3 FT-IR spectrum of complex **3.**

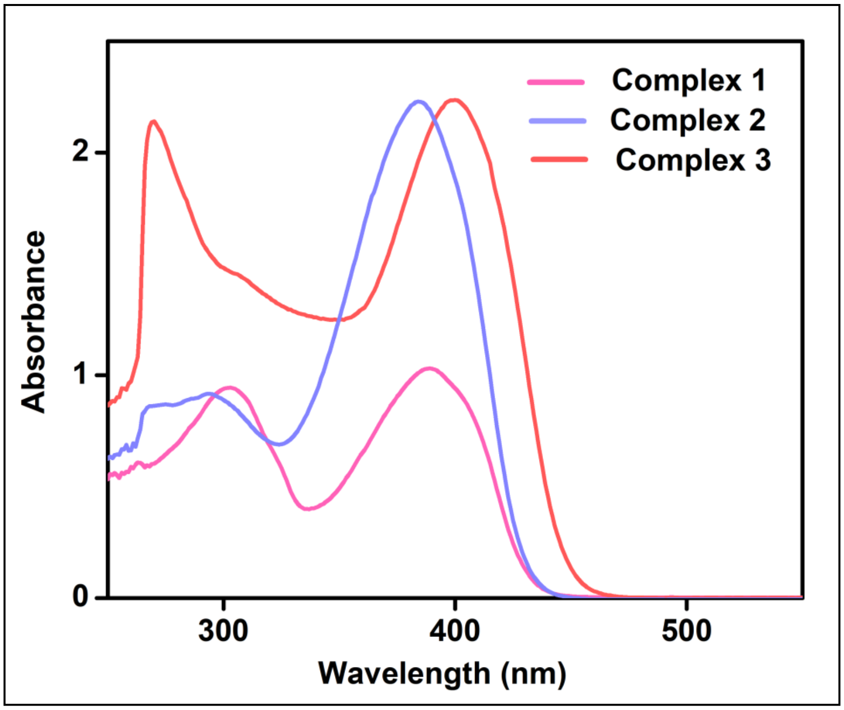

Fig. S4 UV-Vis spectra of complexes **1-3.**

Table S1. Selected Bond Lengths (Å) and Angles (°) of complex 1

Zn(1)-Cl(1)	2.2392(6)	Zn(1)-N(1)	2.1848(13)
Zn(1)-Cl(2)	2.2268(6)	Zn(1)-N(2)	2.0961(12)
Zn(1)-O(2)	2.2636(12)		
Cl(1)-Zn(1)-Cl(2)	116.11(2)	Cl(2)-Zn(1)-N(1)	101.29(4)
Cl(1)-Zn(1)-O(2)	98.94(3)	Cl(2)-Zn(1)-N(2)	135.51(4)
Cl(1)-Zn(1)-N(1)	103.09(4)	O(2)-Zn(1)-N(1)	143.74(4)
Cl(1)-Zn(1)-N(2)	107.78(3)	O(2)-Zn(1)-N(2)	71.45(4)
Cl(2)-Zn(1)-O(2)	94.27(3)	N(1)-Zn(1)-N(2)	74.55(5)

Table S2. Selected Bond Lengths (Å) and Angles (°) of complex 3

Zn(1)-Cl(1)	2.2519(7)	Zn(1)-N(1)	2.132(2)
Zn(1)-Cl(2)	2.2259(8)	Zn(1)-N(2)	2.1284(19)
Zn(1)-O(1)	2.1700(17)		
Cl(1)-Zn(1)-Cl(2)	118.07(3)	Cl(2)-Zn(1)-N(1)	98.93(6)
Cl(1)-Zn(1)-O(1)	98.44(6)	Cl(2)-Zn(1)-N(2)	120.08(5)
Cl(1)-Zn(1)-N(1)	98.17(6)	O(1)-Zn(1)-N(1)	145.82(7)
Cl(1)-Zn(1)-N(2)	121.86(5)	O(1)-Zn(1)-N(2)	72.51(7)
Cl(2)-Zn(1)-O(1)	99.24(5)	N(1)-Zn(1)-N(2)	73.35(7)

Table S3. H-bonding parameters for complex 1

D-H	d(D-H)	d(H..A)	d(D..A)	d(D..A)	A	Symmetry
N(3)-H(3)	0.808(19)	1.977(19)	2.7730(18)	168.4(19)	O(3)	
O(3)-H(3B)	0.8500	2.4600	3.2820(17)	163.00	Cl(1)	1-x,1-y,1-z
O(3)-H(3C)	0.8500	1.8800	2.720(2)	172.00	O(4)	
O(4)-H(4A)	0.8500	2.0900	2.918(2)	165.00	O(2)	x,-1+y, z
O(4)-H(4B)	0.8500	2.3500	3.1494(18)	156.00	Cl(2)	1-x,1-y,-z

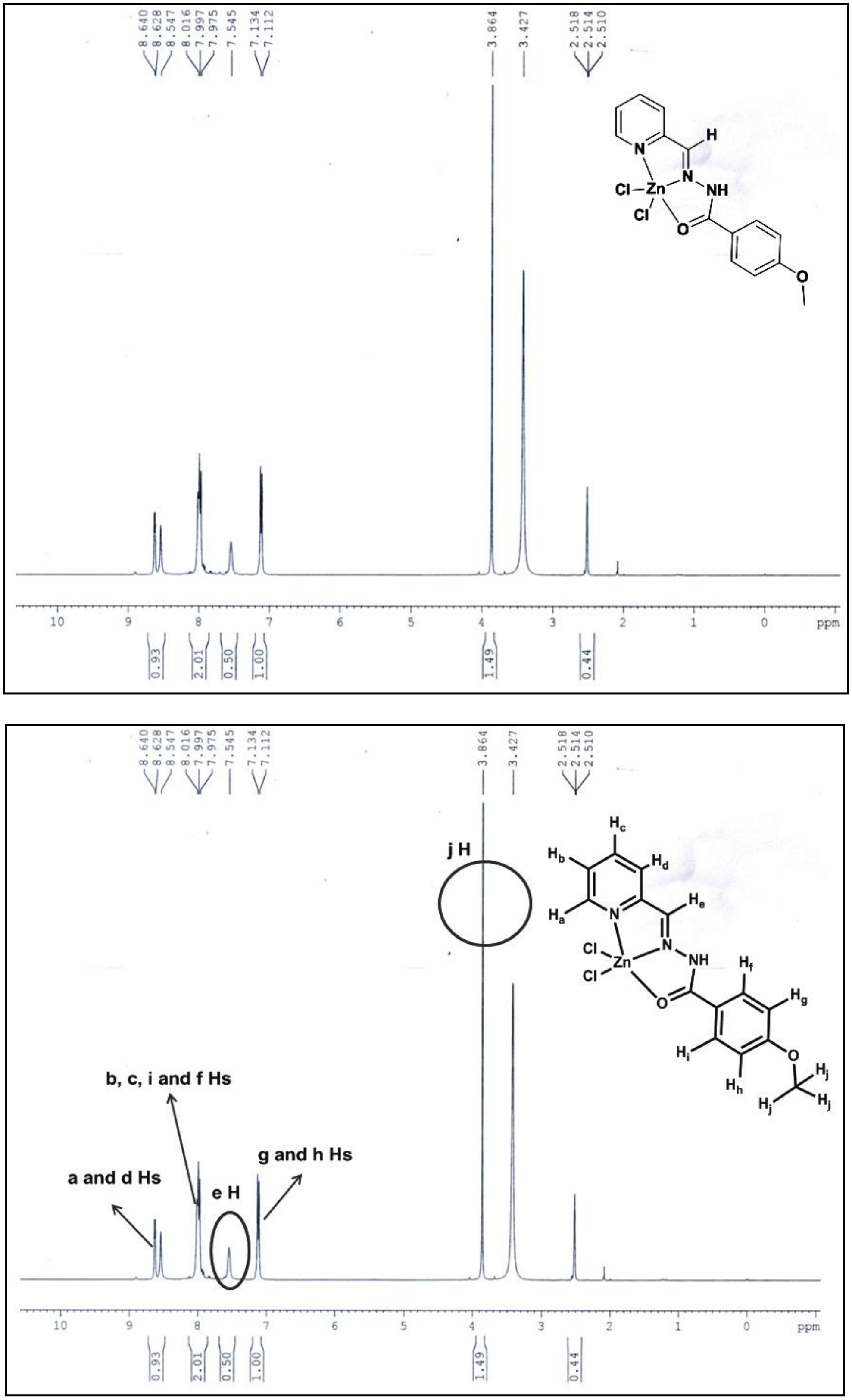

Fig. S5 ^{1}H NMR spectrum of complex **1** recorded in DMSO-d_6 solvent.

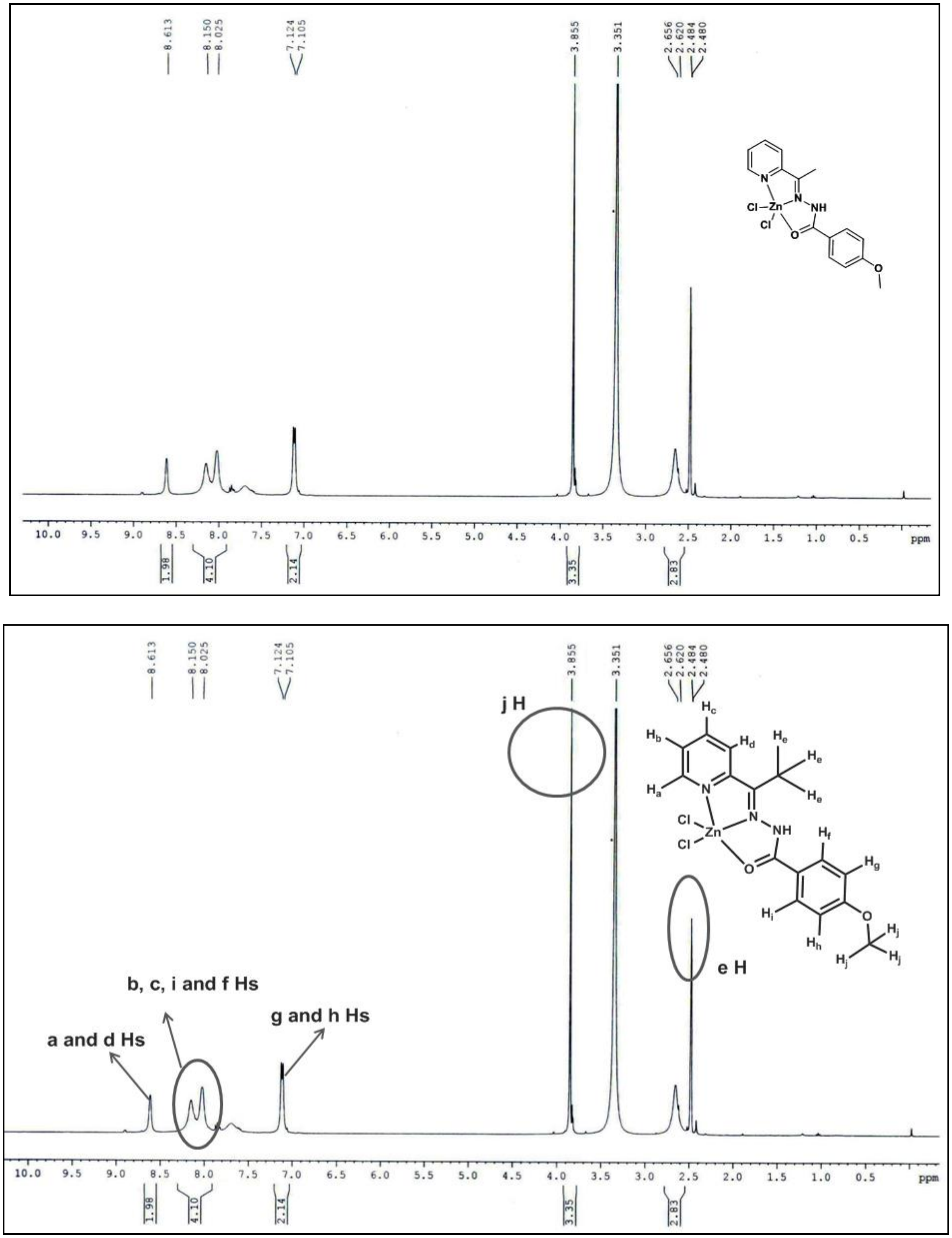

Fig. S6 ^1H NMR spectrum of complex **2** recorded in DMSO-d_6 solvent.

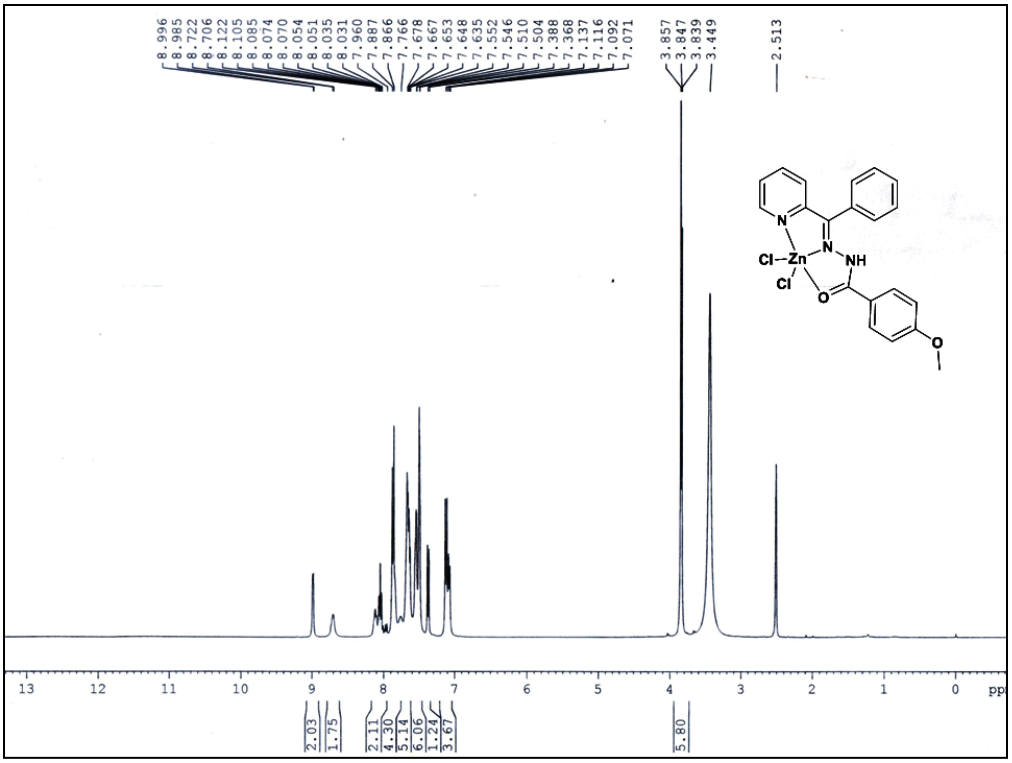

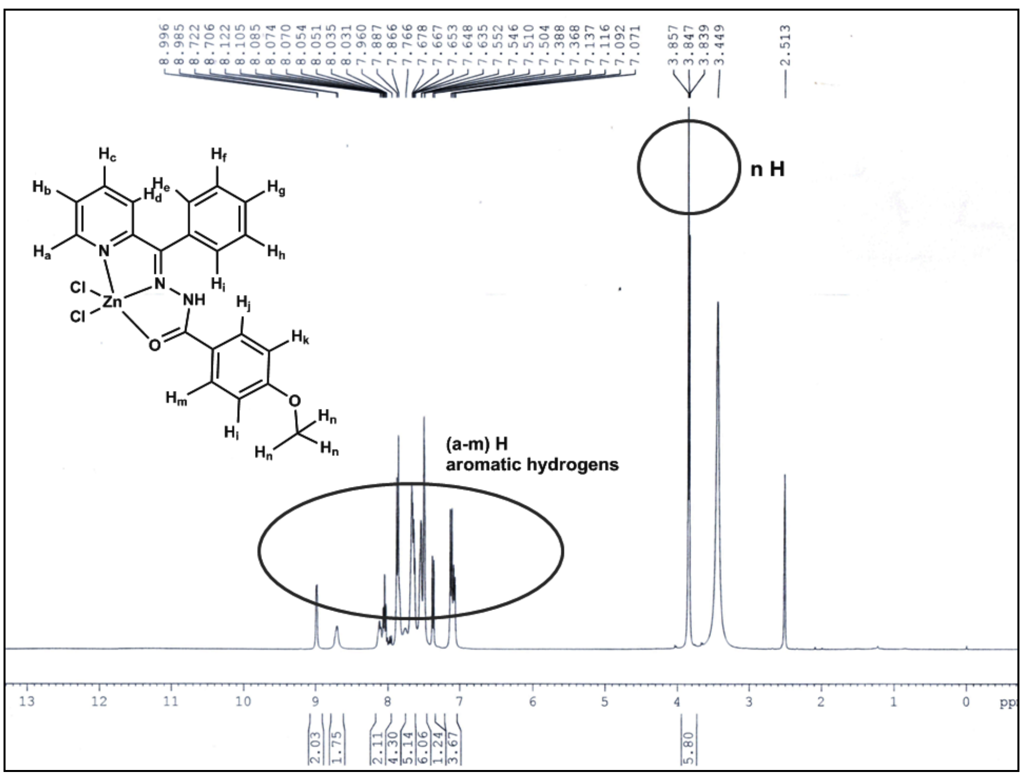

Fig. S7 ^{1}H NMR spectrum of complex **3** recorded in DMSO-d_6 solvent.

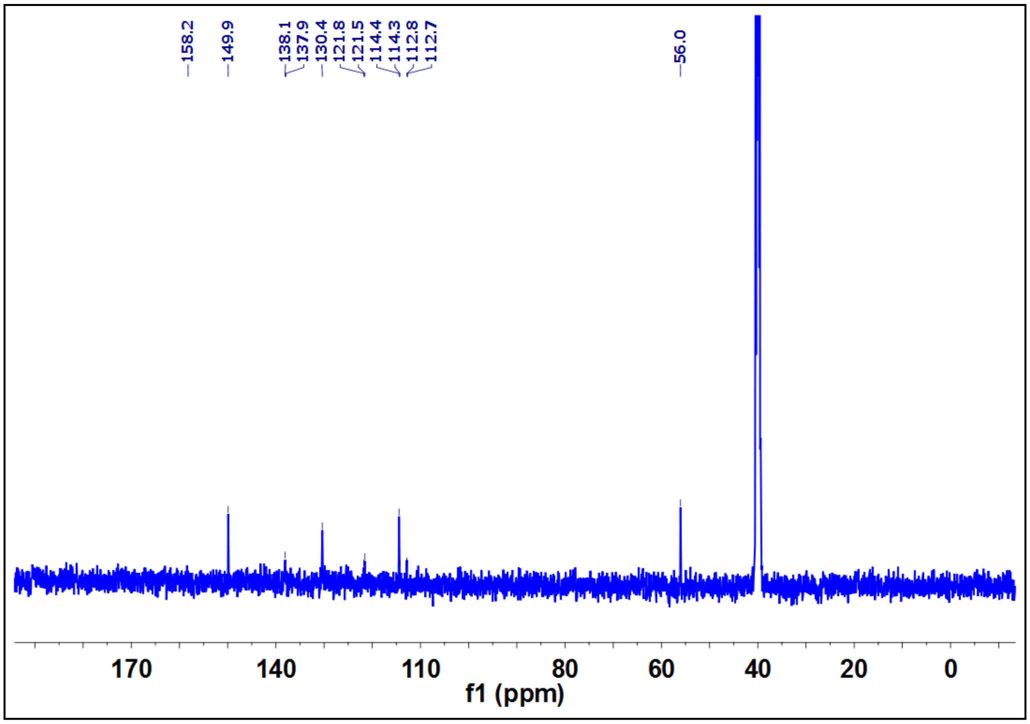

Fig. S8 ^{13}C NMR spectrum of complex **1** recorded in DMSO-d_6 solvent.

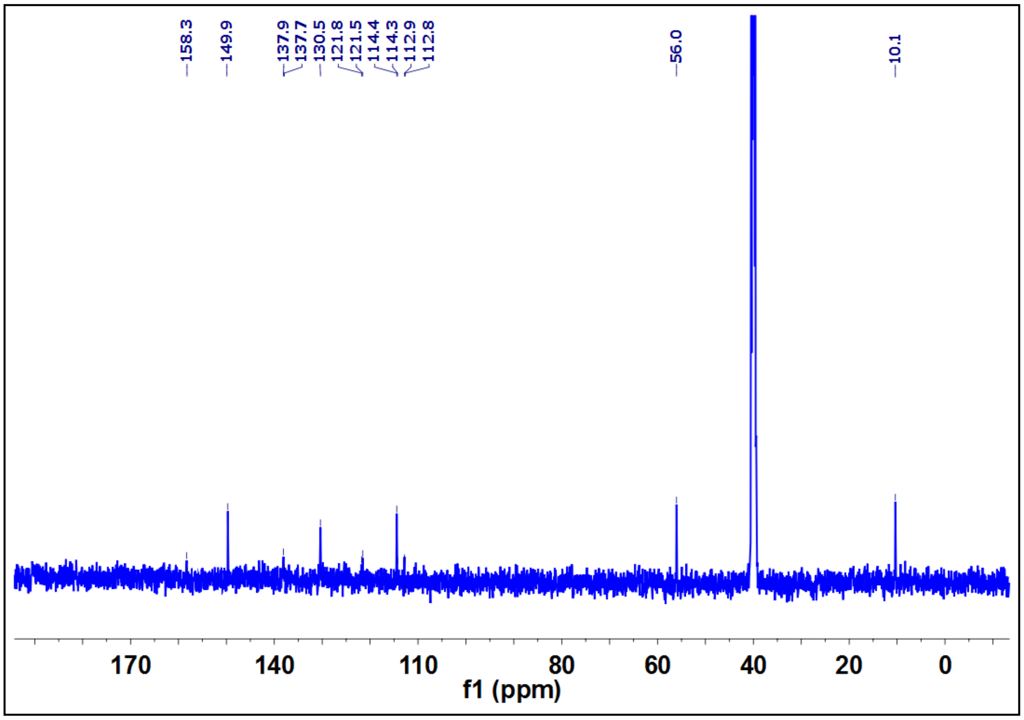

Fig. S9 ^{13}C NMR spectrum of complex **2** recorded in DMSO-d_6 solvent.

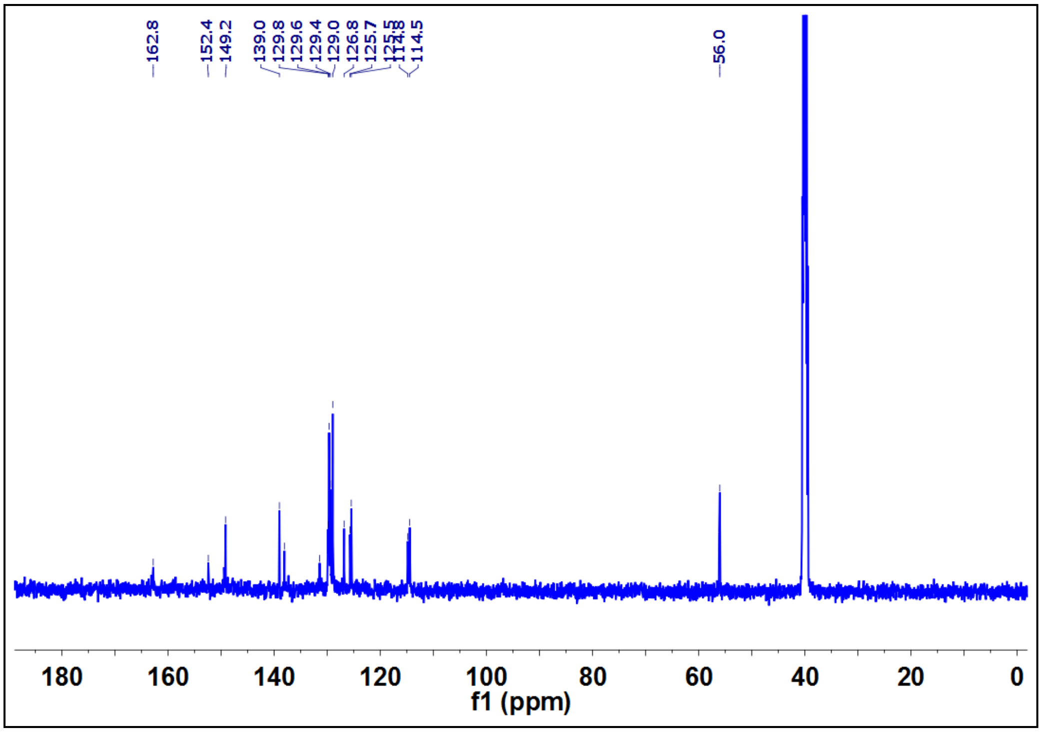

Fig. S10 ^{13}C NMR spectrum of complex **3** recorded in DMSO-d_6 solvent.

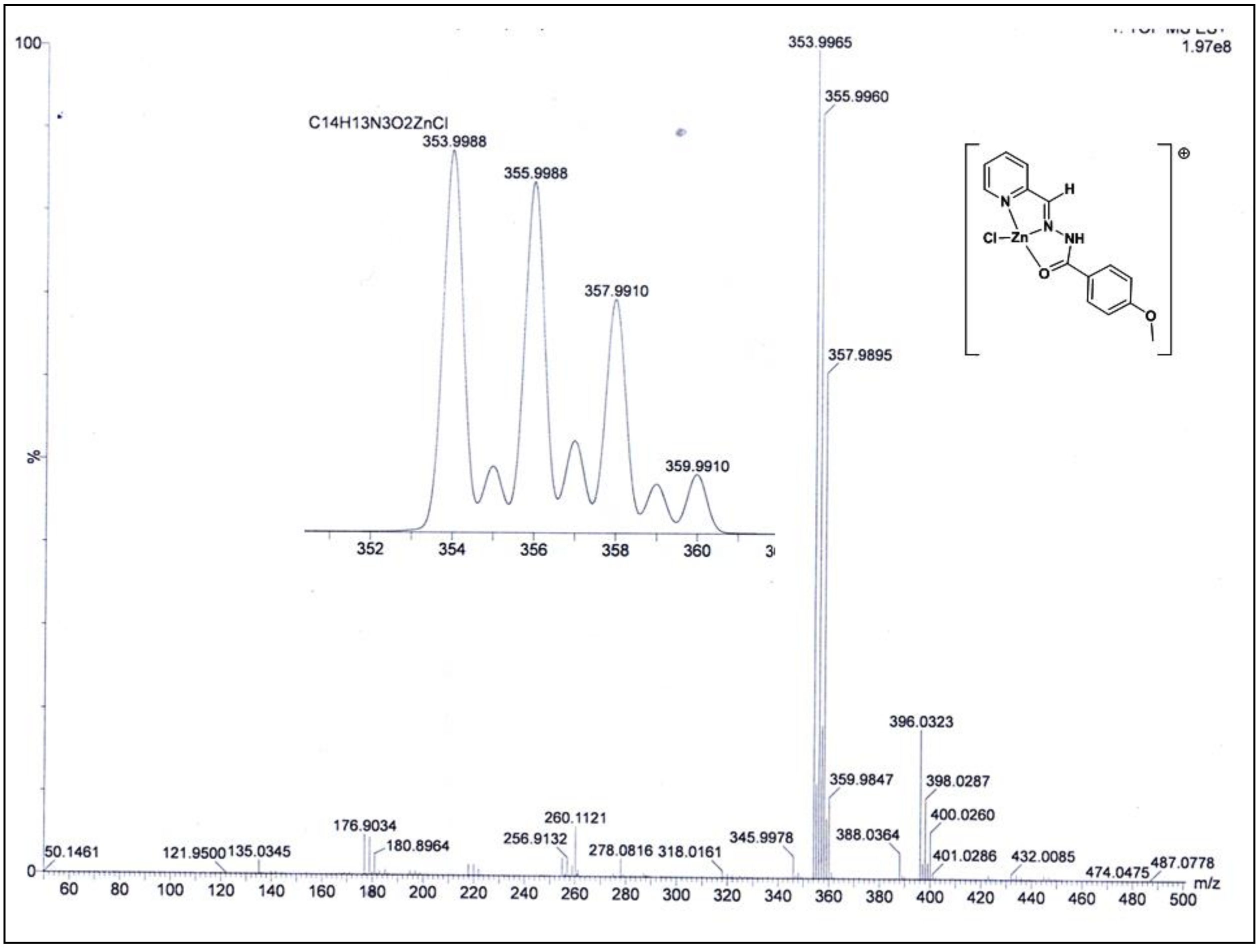

Fig. S11 ESI-MS spectrum of complex **1** in acetonitrile medium recorded in positive mode.

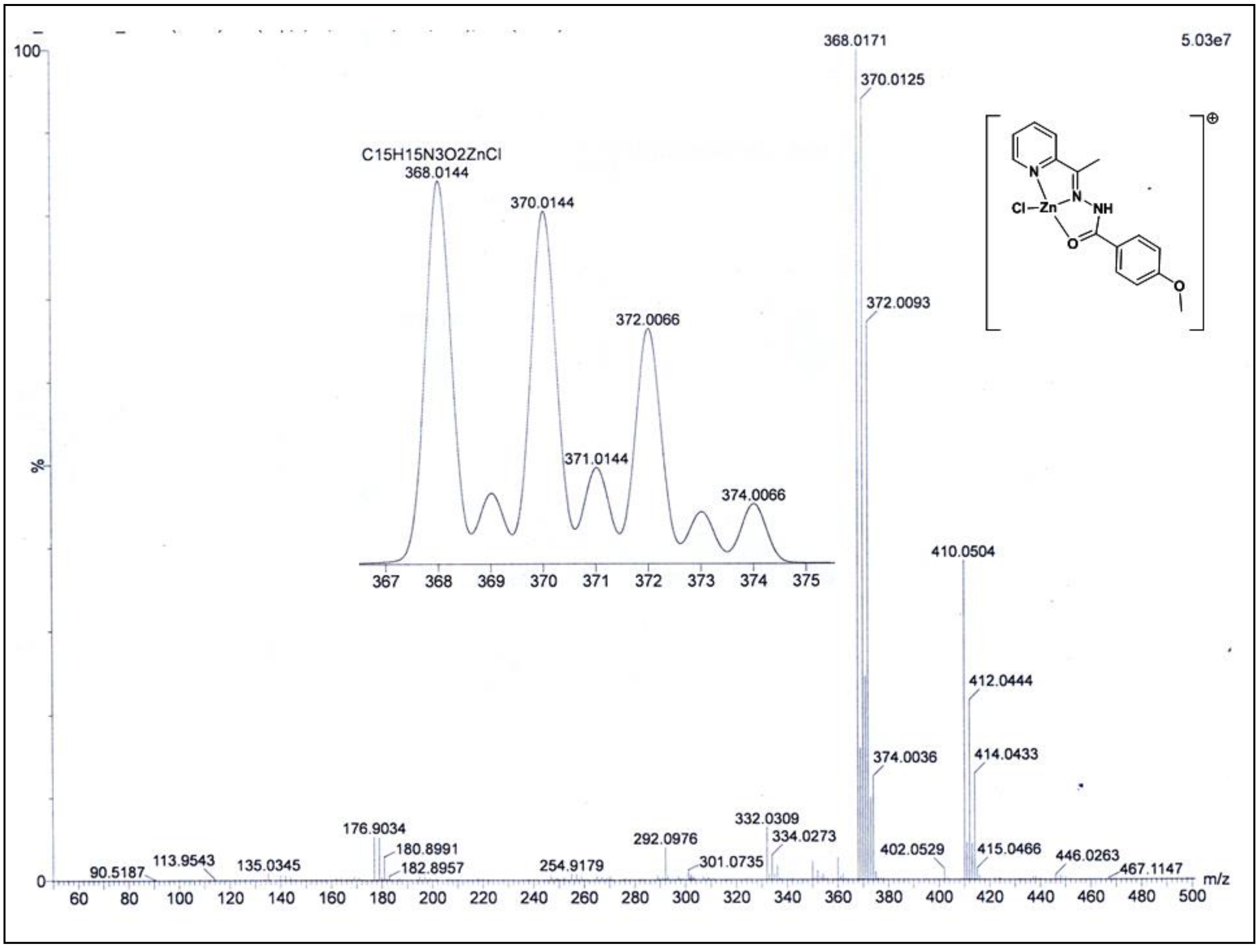

Fig. S12 ESI-MS spectrum of complex **2** in acetonitrile medium recorded in positive mode.

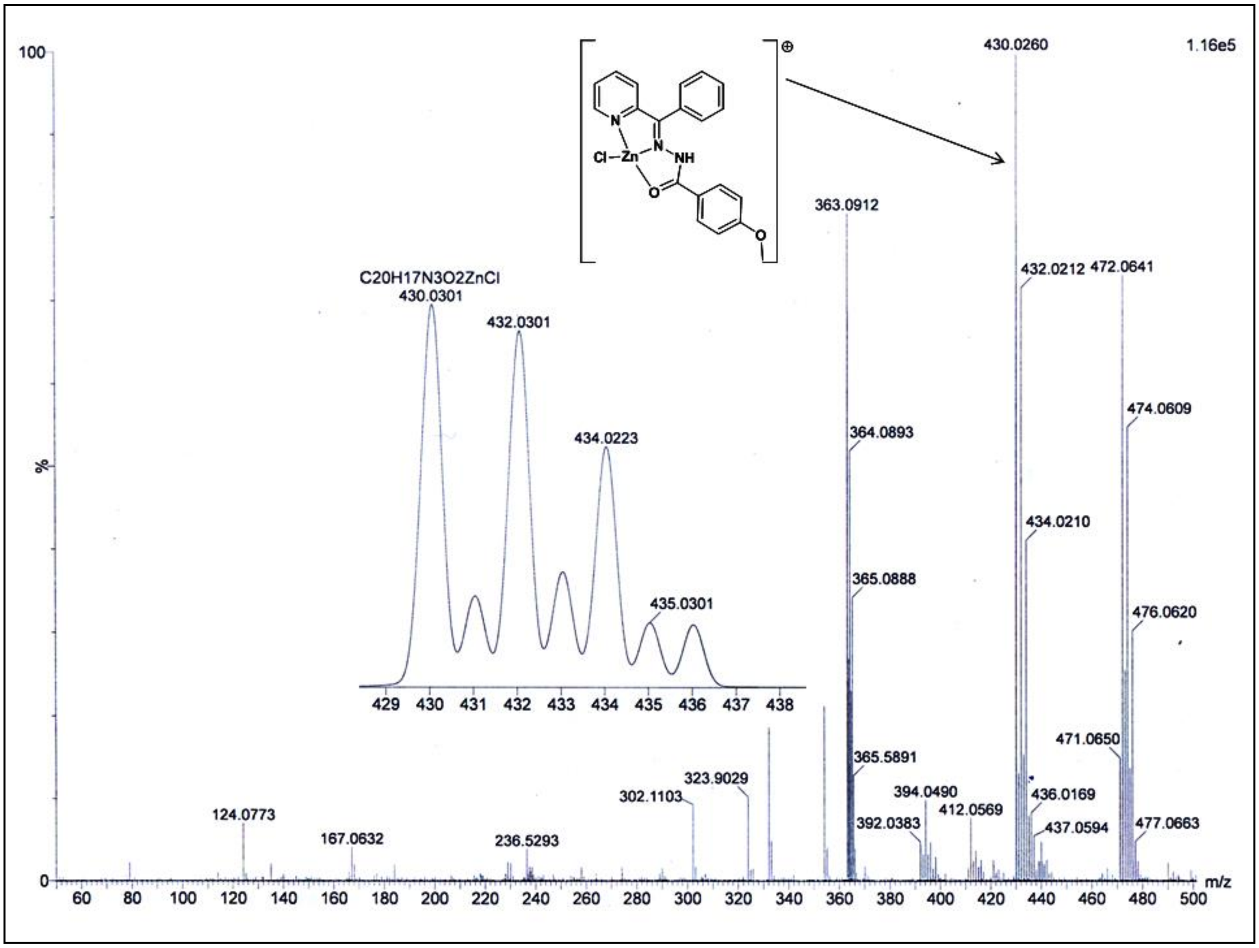

Fig. S13 ESI-MS spectrum of complex **3** in acetonitrile medium recorded in positive mode.

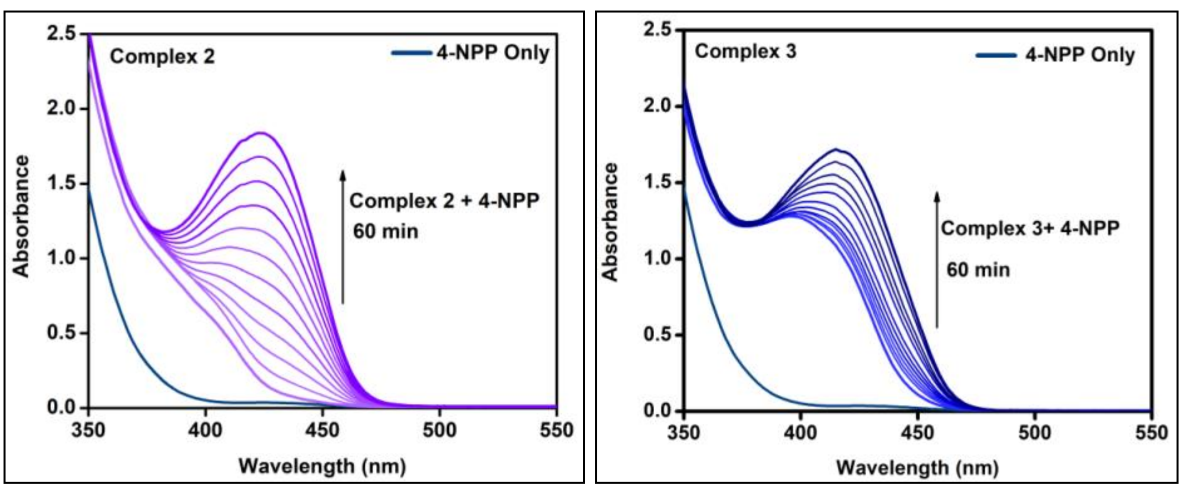

Fig. S14 Wavelength scan for hydrolysis of 4-NPP catalyzed by complex **2** and complex **3** (substrate: catalyst = 20:1) in DMSO-water mixture recorded at 25 °C at intervals of 5 min. [4-NPP] = 1×10^{-3} M;[complex] = 5×10^{-5} M

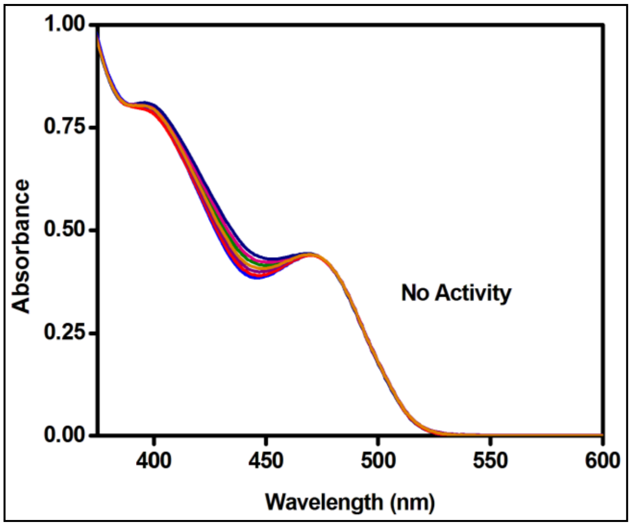

Fig. S15 Controlled experiment of phosphatase activity for zinc(II) chloride in DMSO-water medium at 25°C.

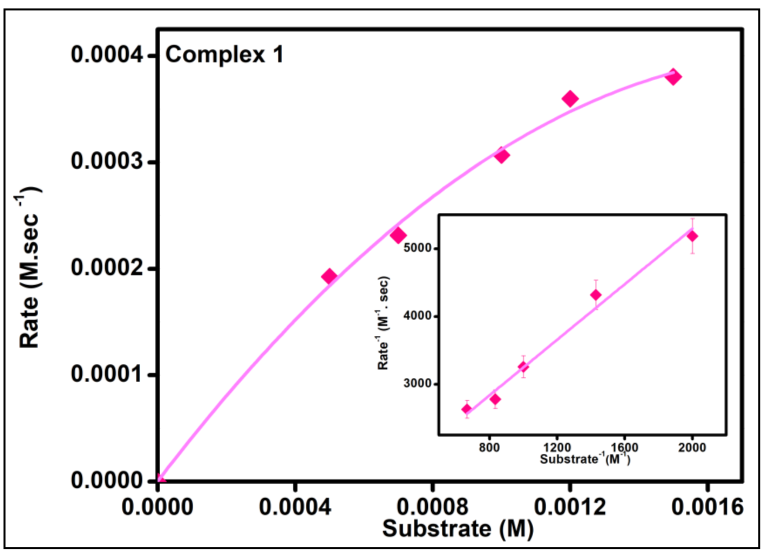

Fig. S16 Dependence of rate of reaction on substrate concentration for complex **1** and inset contains Lineweaver-Burk plots for complex **1** at 25°C in DMSO-water medium for hydrolysis of 4-nitrophenylphosphate.

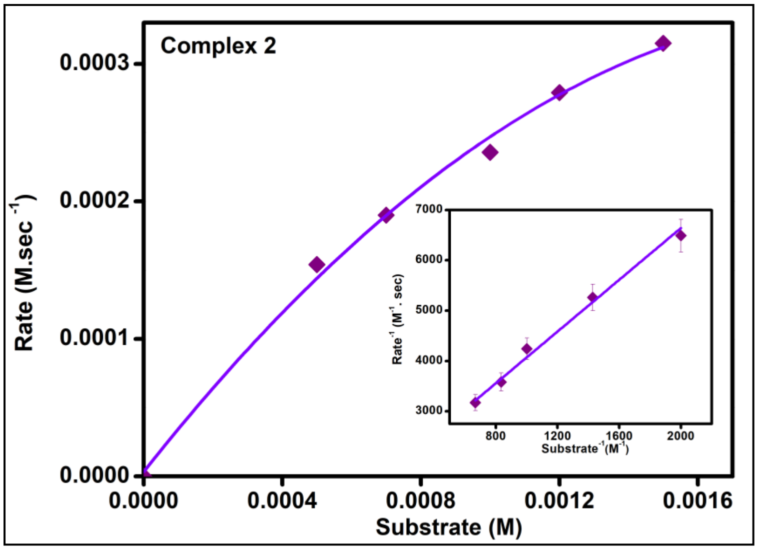

Fig. S17 Dependence of rate of reaction on substrate concentration for complex **2** and inset contains Lineweaver-Burk plots for complex **2** at 25°C in DMSO-water medium for hydrolysis of 4-nitrophenylphosphate.

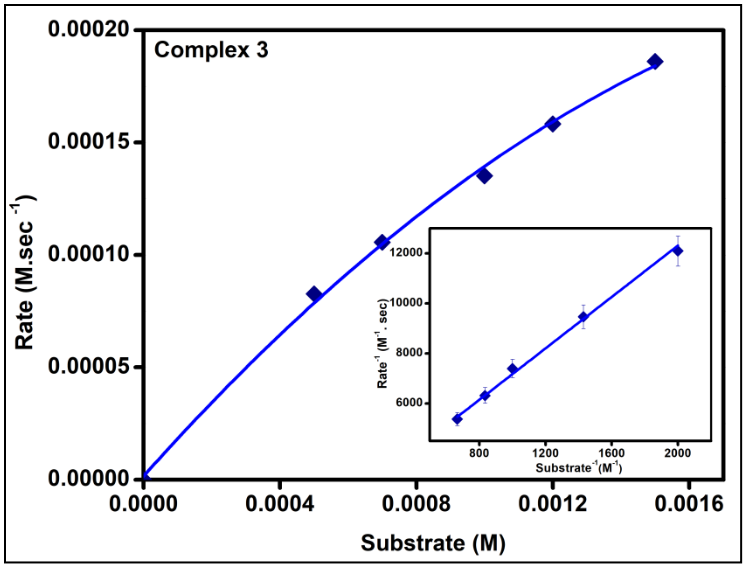

Fig. S18 Dependence of rate of reaction on substrate concentration for complex **3** and inset contains Lineweaver-Burk plots for complex **3** at 25°C in DMSO-water medium for hydrolysis of 4-nitrophenylphosphate.

Table S4. Comparison Table of phosphatase activity of some dinuclear bivalent metal complexes described in literature

Catalyst [a]	Substrate	k_{cat} (s^{-1}) (Solvent)	Ref.[year]
1) $[Zn(L1)Cl_2]\cdot 2H_2O$	PNPP	16.15 s^{-1} (DMSO/H_2O)	Present work
2) $[Zn(L2)Cl_2]$	PNPP	12.52 s^{-1} (DMSO /H_2O)	Present work
3) $[Zn(L3)Cl_2]$	PNPP	9.116 s^{-1} (DMSO/H_2O)	Present work
4) $[Zn_3(L^1)_2(OAc)_4]$	PNPP	7.11×10^{-2} s^{-1} (MeOH/H_2O)	S1[2014]
5) $[Zn(L^2)(OAc)]$	PNPP	4.841×10^{-3} s^{-1} (MeOH/H_2O)	S1[2014]
6) $[Zn_2L^1{}_2Cl_2]$	PNPP	9.35 s^{-1} (DMF/H_2O)	22[2014]
7) $[Zn_2L^1{}_2Br_2]$	PNPP	8.80 s^{-1} (DMF/H_2O)	22[2014]
8) $[Zn_2(L)_2Cl_2]$	PNPP	9.97 s^{-1} (DMF/H_2O)	23[2015]
9) $[Zn_2(L)_2Br_2]$	PNPP	9.47 s^{-1} (DMF/H_2O)	23[2015]
10) $[Zn_2(L)_2I_2]$	PNPP	11.62 s^{-1} (DMF/H_2O)	23[2015]
11) $[Zn_2(L)(SCN)_3]$	PNPP	17.01×10^{-2} s^{-1} (DMF/H_2O)	S2[2017]
12) $[Zn2(LH_{-2})]$	BNPP	2.24×10^{-6} s^{-1} (H_2O)	S3[2002]
13) $[Zn_2(\mu\text{-}L^{Cl}O)(\mu_2\ OAc)_2]\ (PF_6)$	BDNPP	0.48×10^{-3} s^{-1} (MeCN/H_2O)	S4[2016]
14) $[Ni_2(\mu\text{-}L^{Cl}O)(\mu_2\text{-}OAc)_2](PF_6)\cdot 3H_2O$	BDNPP	2.80×10^{-3} s^{-1} (MeCN/H_2O)	S4[2016]
15) $[Zn_2(HL1)(\mu\text{-}OAc)](PF_6)$	BNPP	1.26×10^{-6} s^{-1} (MeCN/H_2O)	S5[2008]
16) $[Zn_2(L^1H_{-1})(OH)](ClO_4)_2$	BNPP	4.9×10^{-6} s^{-1}(DMSO/H_2O)	S6[2005]
17) $[Zn_2(L^2H_{-1})\ (MeOH)\ (OH)]\ (ClO_4)_2$	BNPP	2.3×10^{-5} s^{-1}(DMSO/H_2O)	S6[2005]
18) $[Zn_2(L^2H_{-1})\ (MeOH)\ (OH)]\ (ClO_4)_2$	BNPP	1.9×10^{-6} s^{-1}(DMSO/H_2O)	S7[2004]
19) $[Zn_2(L^4H_{-1})]$	BNPP	4.2×10^{-5} s^{-1}(DMSO/H_2O)	S7[2004]
20) $[Zn_2(BPMP)(\mu\text{-}OH)]^{2+}$	HPNP	6.4×10^{-4} s^{-1}(DMSO/H_2O)	S8[2007]
21) $[Cu_2(L)(\mu\text{-}OH)(H_2O)(ClO_4)_2]$	PNPP	1.69 s^{-1} (DMSO/H_2O)	S9[2015]
22) $[Cu_2\ (L^1)(\mu\text{-}O_2CMe)_2][NO_3]$	HPNP	14.5×10^{-4} s^{-1} (MeOH/H_2O)	S10[2017]
23)$[Cu_4(L)_2(HL)_2(ClO_4)_2]\cdot CH_3OH$	PNPP	9.306 s^{-1} (DMF/H_2O)	25[2019]
24)$[Cu_4(L)_2(HL)_2(NO_3)_2]\cdot C_2H_5OH\cdot 0.5H_2O$	PNPP	7.773 s^{-1} (DMF/H_2O)	25[2019]
25)$[Cu_4(L)_2(HL)_2(OAc)_2]\cdot CH_3CN\cdot H_2O$	PNPP	3.365 s^{-1} (DMF/H_2O)	25[2019]
26) $[Ni_2L^1(CH_3COO)_2(SCN)].(H_2O)_2.(0.5CH_3OH)$	PNPP	8.08×10^{-2} s^{-1}(DMSO/H_2O)	26[2018]
27) $[Ni_2L^2(CH_3COO)(SCN)_2\ (CH_3OH)].(CH_3OH)$	PNPP	5.18×10^{-2} s^{-1}(DMSO/H_2O)	26[2018]

[a]HL^1 (4) = {4-Chloro-2-[(2-morpholin-4-ylethylimino)-methyl]-phenol}
HL^2 (5) = {4-Chloro-2-[(3-morpholin-4-yl-propylimino)-methyl]-phenol}
HL^1(6,7) = 2-((bis(2-methoxyethyl)amino)methyl)-4-methylphenol
HL (8-10) = 2-[bis(2-methoxyethyl)aminomethyl]-4-isopropylphenol
HL(11) = 4-*tert*-Butyl-2,6-bis-[(2-pyridin-2-yl-ethylimino)-methyl]-phenol
LH(12) =1,1′-(1*H*-pyrazole-3,5-diyl)bis(methylene)bis[octahydro-1*H*-1,4,7-triazonine]
HL^{Cl} (13-14) = 2,6-bis[bis(2-pyridylmethyl)aminomethyl]-4-chlorophenol
H_3L1(15) = *N*-(2-hydroxy-3-{[(2-hydroxyethyl)(pyridin-2-ylmethyl)amino]methyl}-5-methylbenzyl)-*N*-(pyridin-2-ylmethyl)aminoacetic acid
L^1(16) = *N*,*N′*-(4*H*-pyrazole-3,5-diyl)bis(methylene)bis{2-(pyridin-2-yl)-*N*-[2-(pyridin-2-yl)ethyl]ethanamine}
L^2(17) = *N*,*N′*-(4*H*pyrazole- 3,5-diyl)bis(methylene)bis{1-(pyridin-2-yl)-*N*-[2-(pyridin-2-yl)ethyl]methanamine}
L^2 (18) = *N1*,*N1′*-(4*H*-pyrazole-3,5-diyl)-bis(methylene)bis{*N1*-[2-(diethylamino)ethyl]-*N2*, *N2*-diethylethane-1,2-diamine}
L^4 (19) = *N1*,*N1′*-(4*H*-pyrazole-3,5-diyl)bis(methylene)bis(*N1*,*N2*,*N2*-trimethylethane-1,2-diamine)
HBPMP (20) = 2,6-bis{[bis(pyridin-2-ylmethyl)amino]methyl}-4-methylphenol
HL(21) = 4-methyl-2,6-bis((*E*)-(6-methyl-1,4-diazepan-6-ylimino)methyl)phenol
HL^1(22) = 4-methyl-2,6-bis((3-(pyridin-2-yl)-1H-pyrazol-1-yl)methyl)phenol
H_2L (23-25) = 4-bromo-2-[(2-hydroxy-1,1-dimethyl-ethylamino)-methyl]-phenol
HL^1(26) =2,6-bis((E)-(2-morpholinoethylimino)methyl)-4-*tert*-butylphenol
HL^2 (27) = 2,6-bis((E)-(2-(piperidin-1-yl)ethylimino)methyl)-4-*tert*-butylphenol]

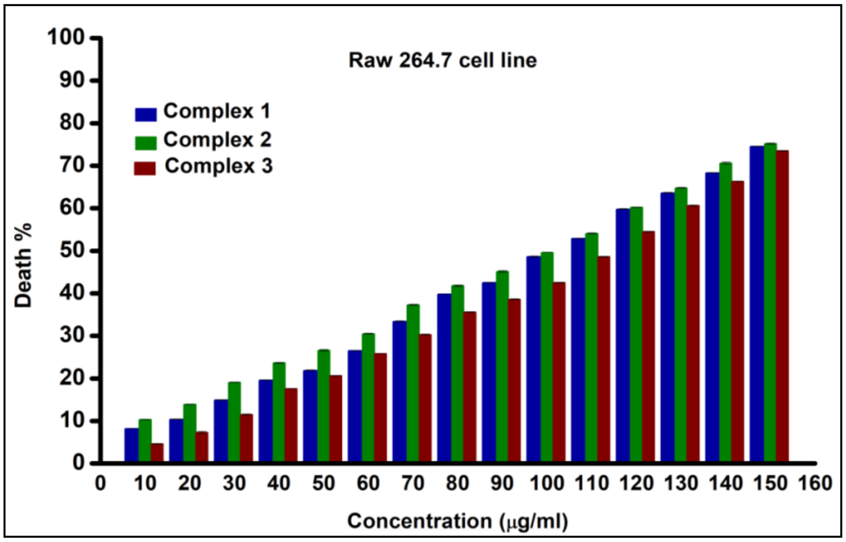

Fig. S19. Cell viability with different concentration (10-150μg/mL) in macrophage cell line (Raw 264.7) for 24 h and cell viability was assayed. Data are delegate as the mean ± SD and are the collective results of three independent experiments.

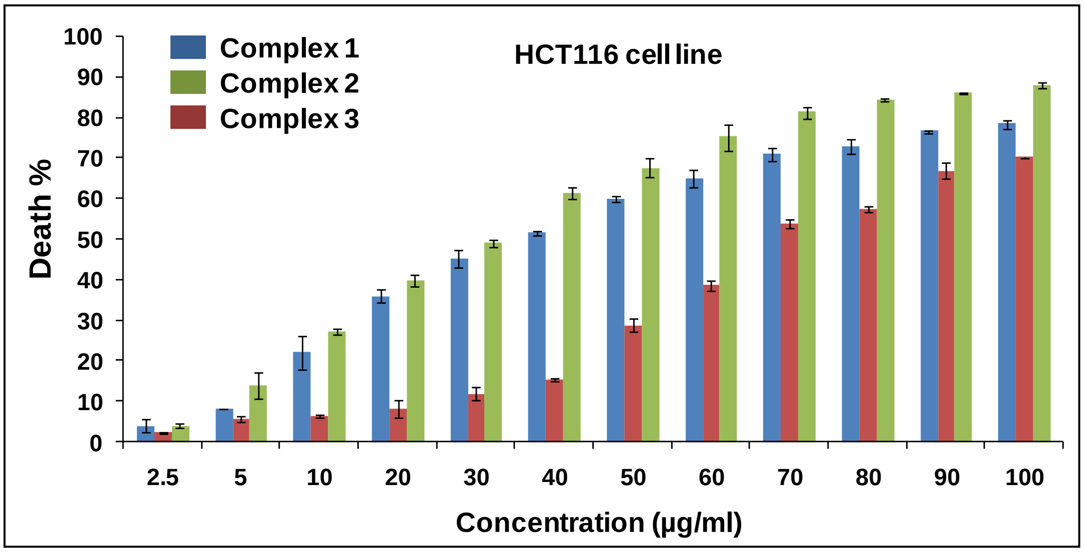

(a)

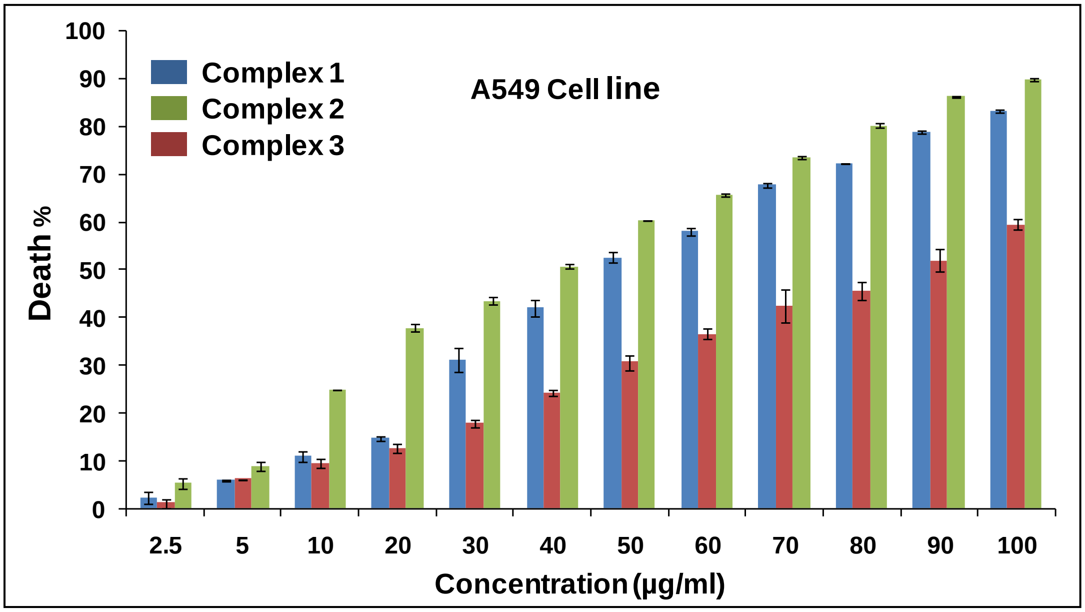

(b)

Fig. S20. Cell viability with different concentration (2.5-100µg/mL) in different cell lines (a) HCT116 (human colorectal carcinoma) and (b) A549 (human non-small lung carcinoma) for 24 h and cell viability was assayed. Data are delegate as the mean ± SD and are the collective results of three independent experiments.

Table S5. Comparison Table of IC_{50} of some previously reported complexes described in literature

Metallodrug [a]	Cell Line	IC_{50}	Ref.^{year}
1) $[Zn(L1)Cl_2]\cdot 2H_2O$	HepG2	31.53 ± 1.6 µg/mL (81.1 µM)	Present work
	A549	48.26 ± 1.7 µg/mL (125 µM)	
	HCT116	43.70 ± 0.56 µg/mL(112.4 µM)	
2) $[Zn(L2)Cl_2]$	HepG2	19.83 ± 1.6 µg/mL (49.2 µM)	Present work
	A549	41.85 ± 0.57 µg/mL (103.8 µM)	
	HCT116	38.66 ± 0.91 µg/mL (95.9 µM)	
3) $[Zn(L3)Cl_2]$	HepG2	66.24 ± 0.38 µg/mL (142.2 µM)	Present work
	A549	87.63 ± 1.8 µg/mL (188.2 µM)	
	HCT116	70.44 ± 1.18 µg/mL (151.3 µM)	
4)*Cis*-platin	HepG2	9.6 ± 2.3µM	42^{2018}
	A549	30±5.0 µM	$S11^{2016}$
	HCT116	25.7 ± 6.3µM	42^{2018}
5)$[Zn_3L^2(\mu\text{-}O_2CCH_3)_2\text{-}(CH_3OH)_4]$	HepG2	70±0.1 µM	$S12^{2014}$
6) Zn(L1)	HepG2	706 µg/mL	$S13^{2014}$
7)aqua[2,2′-[4-methyl-1,2-henylenebis(nitromethylidyne)] dinaphthalato-κ^4 O,N,N′,O′]zinc(II)	HepG2	9.05 µM	$S14^{2013}$
8) [Zn(itpy)(OAc)]-OAc	A549	9.05 µM	$S15^{2014}$
6)$[\{Zn(\mu^2\text{-}H_2O)_{0.5}$ $(5N_3\text{-}IPA)(2,2'\text{-}bpe)\}]_\infty$	HCT116	31.12±1.78 µg/mL	$S16^{2018}$
7) $[\{Zn(\mu^2\text{-}H_2O)_{0.5}$ $(5N_3\text{-}IPA)(1,10\text{-}phen)\}]_\infty$	HCT116	25.56±2.14 µg/mL	$S16^{2018}$
8) $[\{Zn(5N_3\text{-}IPA)(1,2\text{-}bpe)\}]_\infty$	HCT116	25.75±1.14 µg/mL	$S16^{2018}$
9)$[\{Zn(5N_3\text{-}IPA)(1,2\text{-}bpey)\}]_\infty$	HCT116	31.96±1.54 µg/mL	$S16^{2018}$
10)$[\{Zn(H_2O)$ $(5N_3\text{-}IPA)$ $(4,4'\text{-}tme)\}$ $(H_2O)_{0.5}]_\infty$	HCT116	33.98±1.47 µg/mL	$S16^{2018}$
11) [Ru(hmb)(L1)Cl]	HCT116	115 ± 25 µM	42^{2018}
	HepG2	>200 µM	42^{2018}
12) [Ru(cym)(L1)Cl]	HCT116	113 ± 40 µM	42^{2018}
	HepG2	>200 µM	42^{2018}
13) [Ru(hmb)(L2)Cl]	HCT116	>200 µM	42^{2018}
	HepG2	>200 µM	42^{2018}
14)[Ru(cym)(L2)Cl]	HCT116	175 ± 10 µM	42^{2018}

	HepG2	>200 µM	42[2018]
15)[Ru(hmb)(L3)Cl]	HCT116	>200 µM	42[2018]
	HepG2	>200 µM	42[2018]
16)[Ru(cym)(L3)Cl]	HCT116	163 ± 20 µM	42[2018]
	HepG2	>200 µM	42[2018]

[a]H_2L (5) = 2-[(2-hydroxyphenylimino)methyl]-6-methoxyphenol
L1 (6) = 4-chloro-2-(((4-morpholinophenyl)imino)methyl)phenol
itpy (8) = 4'-(1H-imidazol-2-yl)-2,2':6',2''-terpyridine
$5N_3$-IPA (5-9) = 5-azidoisophthalic acid
HL1(11-12) = 2-((5-hydroxo-3-methyl-1-phenyl-1H-pyrazol-4-yl)(phenyl)methylene)-1-(2,4-nitrophenyl)hydrazine
HL2 (13-14) = 2-((5-hydroxo-3-methyl-1-phenyl-1H-pyrazol-4-yl) (phenyl)methylene)-1-(4-nitrophenyl)-Hydrazine
HL3 (15-16)= 2-((5-hydroxo-3-methyl-1-phenyl-1Hpyrazol-4-yl)(phenyl)methylene)-1-(pyridin-2-yl)hydrazine)

References.

S1 P. Chakraborty, J. Adhikar, R. Sanyal, A. Khan, K. Manna, S. Dey, E. Zangrando, A Bauzá, A. Frontera, D. Das, *Inorg. Chim. Acta.*, 2014, **421**, 364.

S2 J. Adhikary, P. Chakraborty, S.Samanta, E. Zangrando, S. Ghosh, D. Das, *Spectrochim. Acta A.* 2017, **178**, 114

S3 C. Vichard, T. A. Kaden, *Inorg. Chim. Acta* 2002, **337**, 173.

S4 S. S. Massoud, C. C. Ledet, T. Junk, S. Bosch, P. Comba, R. Herchel, J. Hošek, Z. Trávníček, R. C. Fischerd , F. A. Mautner, *Dalton Trans*. 2016, **45**, 12933.

S5 R. R. Buchholz, M. E. Etienne, A. Dorgelo, R. E. Mirams, S. J. Smith, S. Y. Chow, L. R. Hanton, G. B. Jameson, G. Schenk, L. R. Gahan, *Dalton Trans.* 2008, 6045.

S6 B. Bauer-Siebenlist, F. Meyer, E. Farkas, D. Vidovic, S. Dechert, *Chem. Eur. J.* 2005, **11**, 4349.

S7 B. Bauer-Siebenlist, F. Meyer, E. Farkas, D. Vidovic, J. A. Cuesta-Seijo, R. Herbst-Irmer, H. Pritzkow, *Inorg. Chem.* 2004, **43**, 4189.

S8 K. Selmeczi, C. Michel, A. Milet, I. Gautier-Luneau, C. Philouze, J.-L. Pierre, D. Schnieders, A. Rompel, C. Belle, *Chem. Eur. J.* 2007, **13**, 9093.

S9 I. Majumder, P. Chakraborty, S. Das, H. Kara, S. K. Chattopadhyay, E. Zangrando, D. Das, *RSC Adv.*, 2015,**5**, 51290

S10 N.A. Rey, A. Neves, A.J. Bortoluzzi, C.T. Pich, H.Terenzi, *Inorg. Chem.* 2007, **46**, 348.

S11 P. Baharuddin, N. Satar, K. S. Fakiruddin, N. Zakaria, M.N. Lim, N. M. Yusoff, Z. Zakaria , B. H. Yahaya, *Oncology Rep*. 2016, **35**,13.

S12 D. Dey, G. Kaur, A. Ranjani, L. Gayathri, P. Chakraborty, J. Adhikary, J. Pasan, D. Dhanasekaran, A. R. Choudhury, M. A. Akbarsha, N. Kole, B. Biswas, *Eur. J. Inorg. Chem.*2014, 3350.

S13 K. Dhahagani, S. Mathan Kumar , G. Chakkaravarthi, K. Anitha, J. Rajesh, A. Ramu, G. Rajagopal, *Spectrochim. Acta A*, 2014, **117** , 87.

S14 A. M. Farag, T. S. Guan, H. Osman, A. M. S. A. Majid, M. A. Iqbal, M. B. K. Ahamed, *Med Chem Res*, 2013, **22**, 4727.

S15 V. M. Manikandamathavan, T. Weyhermüller, R. P. Parameswari, M. Sathishkumar, V. Subramaniana, B. U. Nair, *Dalton Trans.*, 2014, **43**,13018.

S16 S. Mukherjee, S. Ganguly, K. Manna, S. Mondal, S. Mahapatra, D. Das, *Inorg. Chem.* 2018, **57**, 4050